© SEP 2021 | IRE Journals | Volume 5 Issue 3 | ISSN: 2456-8880

Armature Regulation of DC Motor Using PI Controlled DC-DC Flyback Converter

M.J. DESHI[1], E.C. ANENE[2], E.E. OMIZEGBA[3]
[1] *M.Eng. Student, Department of Electrical and Electronics Engineering A.T.B.U Bauchi, Nigeria*
[2, 3] *Prof., Department of Electrical and Electronics Engineering A.T.B.U Bauchi, Nigeria*

Abstract- Electricity supply obtained from DC sources like photovoltaic cells is not usually compatible with nominal bias voltage requirement for most appliances, hence the need for voltage conversion. One of such converters is the flyback converter system. The flyback converter is a DC-DC converter capable of stepping up or stepping down DC voltage while providing galvanic isolation between its input and output sides. In this work, a flyback converter system is designed using the Amp and Volts seconds balance equations on the state space model. The designed system deployed a PI controller having gains obtained from classical root locus technique implemented in MATLAB SISOTOOL. The flyback converter circuit design considered a strategy that handles undesirable surge current during switching transitions so as to protect the circuit. It was demonstrated that by keeping the armature voltage constant, the DC Motor will run at constant speed even when acted upon by a variable load provided the load is not beyond the capacity of the motor. Also varying the armature voltage will ensure that DC motor runs at variable speed. The step response analysis of the closed loop-controlled system shows that a rise time of 0.7ms and a peak overshoot of 5.11% were achieved giving the system a faster and stable response.

Indexed Terms- Armature, Flyback Converter, DC-Motor, Torque, PI Controller, Speed, State Space.

I. INTRODUCTION

With advancement in power electronics, switch mode power converters became very popular and more efficient[1]. Switched-mode DC-DC power converters changes one DC voltage level to another, which may be larger or smaller, by accumulating the input energy temporarily and then discharging that energy to the output at a dissimilar voltage in the later stage [2]. The storehouse may be in either magnetic field storage element (inductors or transformers) or electric field storage elements (capacitors). A substantial upgrade in switch mode DC-DC converters can be achieved by replacing the flywheel diode by synchronous rectification using a power FET, whose "on resistance" is much lower thereby reducing switching losses [3]. There exist different types of switch mode power converter each having different kind of control schemes in use and with the increase in circuit complexity for accurate and improved technology a more severe requirement for accurate and fast regulation can be achieved. One of the most commonly used switch mode power converter is the flyback converter. The flyback converter is a constant output power switching converter. It is mostly useful for multiple output application where a more stringent output voltage tracking is required than most other switching topologies[4]. The flyback converter is a modification of a buck–boost converter using one switch [5]. The converter is widely used in robotics industries to power DC motors, as a battery charge controller in photo voltaic systems, powering of digital devices such as computers and in most modern laptops and cell phones charger etc. The flyback converter is a non-minimum phase system having a zero on the right hand side of the S-plane and by root locus analysis a pole must terminate at a zero for a varying gain which imply that it naturally an unstable system [6]. The control strategy for the stability of the flyback converter has been a subject of research.

According to [7], one way of converting a DC voltage to another DC of different level is by using a Pulse Regulation which is a fixed frequency control technique that is introduced and applied to flyback converter operating in discontinuous conduction mode (DCM). [5] Presented a simplified approach for flyback converter for armature control DC motor drive using a single–phase, single-way diode bridge rectifier in cascade with the flyback converter. A digital signal processor (DSPdspace1102) board was used to implement the converter in open and closed-loop and accordingly, a step-down and step-up characteristic of the output voltage was obtained. This technique provides a ripple free output voltage and current. Fuzzy controller has been used to implement a flyback converter for DC motor armature control[8]. This is done to provide efficient method to control the speed of DC motor using analog controller. The fuzzy controller does not use complex mathematical model and also provides a better way to models to implement good control strategy. [3] Investigated a flyback converter with a new non complementary active clamp control method to achieve soft switching and high efficiency for heavy motor load and light load conditions. This is quite attractive for low power application with universal ac inputs, such as external adaptors. With this topology, the energy in the leakage inductance can be fully recycled there by increasing the efficiency of the converter. However, the conventional complementary gate signal and constant frequency (CF) control method result in poor efficiency at light-load condition, which lowers the average efficiency. Author in [9] designed and implement a single phase single switch DC-DC flyback converter with isolation using PID controller to control a DC motor. It was stated that the converter is cost effective because its components count was less when compare with other topology. [10] designed a flyback converter working with buck-boost regulator which is fed from the energy generated by renewable sources like solar and wind energy to control an electric vehicle. This system was implemented using a six phase generator to generate the power from the wind fans and then six phase converter (rectifier) was used to convert the generated AC to DC. The use of fly-back converter in the power conversion system ensures that the ripple voltage was minimized and used to drive the electric vehicle.

II. SYSTEM DESIGN AND MODEL

The system block consists of AC-DC converter with over current and inrush current protection to convert the high input mains to high DC voltage followed by a flyback converter with an incorporated PI controller to step down the high DC voltage to 12V which is compatible with the DC motor requirement as shown by the block description of Fig.1.

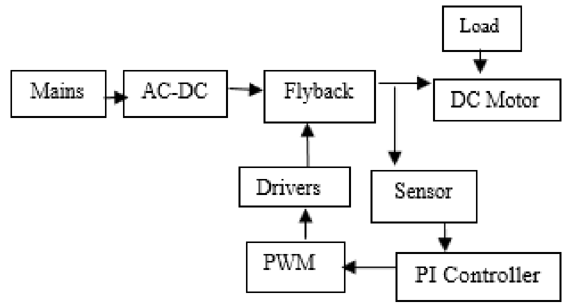

Fig 1: The System Block Diagram

A. Design and Analysis of AC-DC Converter with Over Current and Inrush Protection Circuit

In the work as seen in Fig.2 delay circuit is designed to limit the inrush current and a diode bridge rectifier was used to convert the AC mains to pulsating DC filtered using a bulk power capacitor to obtain a smooth DC supply. The MOSFET, the BJT and the biasing resistors constituted the over current and inrush protection circuit.

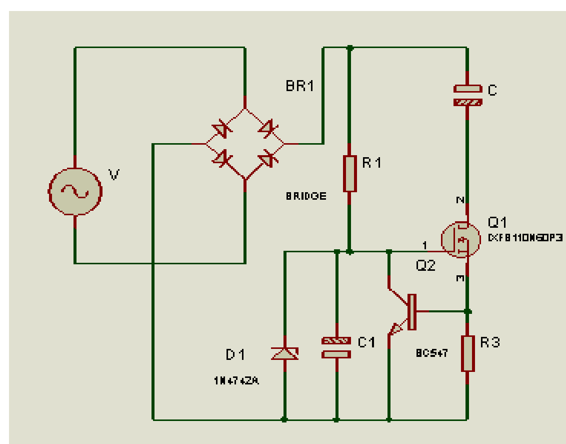

Fig 2: AC-DC Converter with over Current and Surge Protection

Table 1 gives the design specifications of the AC-DC converter

Table 1: AC-DC Converter Input Specifications

Specification	Symbol	Value	Units
Minimum input peak voltage	v_{min}	120	V

Maximum input peak voltage	v_{max}	400	V
Ripple factor	Δv	5	%
Average output current	i_o	0.3	A
Mains frequency	f	50	Hz

The filter capacitor is computed from:

$$c = i_o\left(\frac{\pi-\alpha}{\pi}\right)\frac{1}{2f\Delta v} \quad \ldots(1)$$

Where $\alpha = \cos^{-1}\left(\frac{v_{min}}{v_{max}}\right)$

The diode peak inverse voltage, its average current and the output current are given by:

$$\text{Diode PIV} = 2v_{in} \quad \ldots(2)$$

$$i_d ave = \frac{i_m\alpha}{2\pi} \quad \ldots(3)$$

$$i_o = \frac{i_m\alpha}{\pi} \quad \ldots(4)$$

Table 2 shows the design specifications needed to design the over current and inrush current circuit

Table 2: Design Specifications for Protection Circuit

Specification	Symbol	Value	Units
Initial gate voltage	v_i	0	V
Gate threshold voltage	v_{gsth}	4	V
Final gate voltage	v_f	12	V
Full voltage ON time	t	120	ms
Minimum input voltage	$v_{f\,min}$	76	V
Maximum input voltage	$v_{f\,max}$	225	V

By selecting the value of the capacitor C_1 the resistor R_1 is obtained as:

$$R_1 = \frac{t}{C_1 \ln\frac{v_f}{v_f - v_i}} \quad \ldots(5)$$

B. The Flyback Converter

Flyback converters are designed for continuous-current operation to give smoother output. The choice of the converter switching frequency and inductance associated with the switching transformer to give continuous current is important. As the switching frequency increases, the minimum size of the transformer inductance to produce continuous current and the minimum size of the capacitor to limit output ripple both decrease[11]. Therefore, high switching frequencies are desirable to reduce the size of the reactive components. The tradeoff for high switching frequencies is increase in power loss in the switching device.

The schematic of the flyback converter is as shown in Fig.3

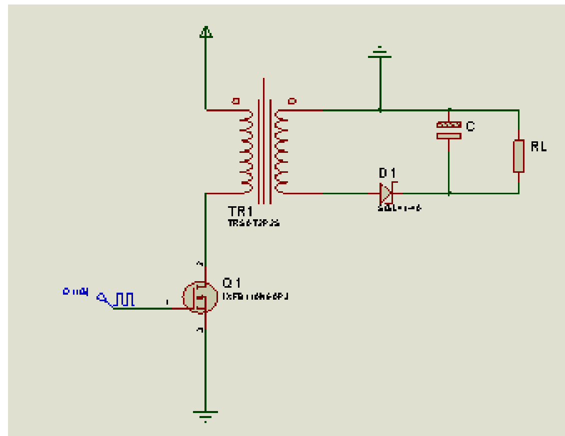

Fig 3: The Flyback Converter

The flyback converter was designed based on the input specification of Table 3.

Table 3: Flyback Converter Design Specifications

Specifications	Symbol	Value	Units
Turns ratio	n	0.3	-
Ripple factor	Δv	10	%
Switching frequency	f_s	80	KHz
Output voltage	v_0	12	V
Min. peak input voltage	v_{min}	120	V
Max. peak input voltage	v_{max}	400	V
Change in inductor current	Δi	10	%
Output current	i_0	3	A

From Fig.3, the primary magnetizing inductance and the output capacitor are given by:

$$L = \frac{v_{in}DT_S}{\Delta i} \quad \ldots(6)$$

$$C = \frac{i_o D}{\Delta v f_S} \quad \ldots(7)$$

The duty cycle of the converter is selected to be less than 50% to reduce the switching stress

The sensor employed for the flyback converter is the optocoupler as shown in Fig.4. This is selected to ensure that the galvanic isolation between the input and the output of the converter is maintained.

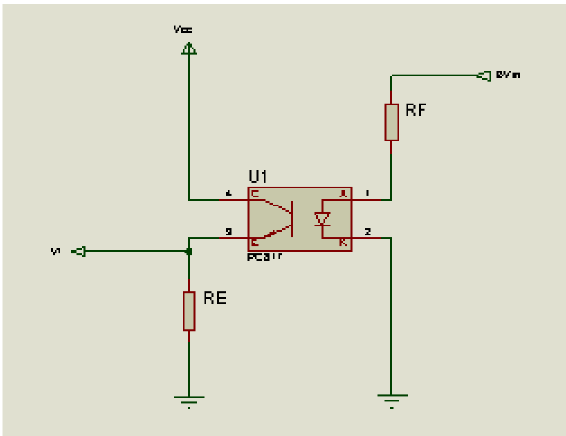

Fig 4: The Optocoupler Sensor

Referring to Fig.4, the feedback resistor and the emitter stabilization resistor are obtained as:

$$R_f = \frac{\beta v_o - v_D}{i_f} \qquad \ldots(8)$$

$$R_E = \frac{v_f}{i_E} \qquad \ldots(9)$$

Where β is the feedback factor, i_f is the forward current and i_E is the emitter current

The pulse width modulator is designed using the switch mode power supply controller integrated circuit UC3843. It has an inbuilt high gain error amplifier, two comparators, an RS latch and a totem pole output suitable for driving a power MOSFET directly as shown in Fig.5

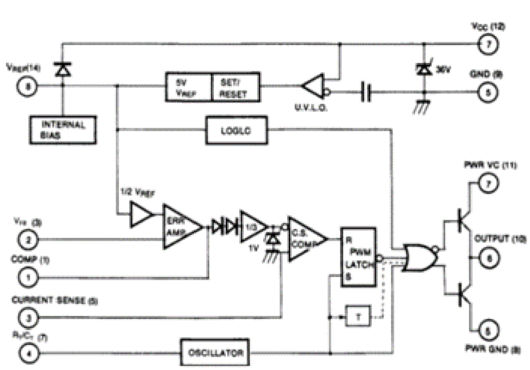

Fig 5: The Switch Mode Power Supply Controller

The oscillator was programmed to switch at a frequency which is given by;

$$f = \frac{1.8}{R_T C_T} \qquad \ldots(10)$$

for $R_T > 5K$

C. System Modeling

From Fig.3, when the power MOSFET is turned ON, the input voltage comes directly across the magnetizing inductance of the switching transformer with respect to the dot convention, a voltage will be induced on the secondary side in a manner such that it reverse biases the diode so that field energy is stored in the core giving rise to the to the dynamics given by:

$$\begin{pmatrix} \dot{i}_L \\ \dot{v}_c \end{pmatrix} = \begin{pmatrix} 0 & 0 \\ 0 & -\frac{1}{RC} \end{pmatrix} \begin{pmatrix} i_L \\ v_c \end{pmatrix} + \begin{pmatrix} \frac{1}{L} \\ 0 \end{pmatrix} v_{in} \qquad \ldots(11)$$

$$v_o = \begin{pmatrix} 0 & 1 \end{pmatrix} \begin{pmatrix} i_L \\ v_c \end{pmatrix} \qquad \ldots(12)$$

When the switch is OPEN, the magnetic field decays and there will be a reversal in polarity in a manner that all the energy is transferred to the output side to charge the capacitor and supply the load, changing the dynamics to:

$$\begin{pmatrix} \dot{i}_L \\ \dot{v}_c \end{pmatrix} = \begin{pmatrix} 0 & \frac{d-1}{nL} \\ \frac{1-d}{nC} & -\frac{1}{RC} \end{pmatrix} \begin{pmatrix} i_L \\ v_c \end{pmatrix} + \begin{pmatrix} \frac{d}{L} \\ 0 \end{pmatrix} v_{in} \qquad \ldots(13)$$

$$v_o = \begin{pmatrix} 0 & 1 \end{pmatrix} \begin{pmatrix} i_L \\ v_c \end{pmatrix} \qquad \ldots(14)$$

The average of (11) and (13) and that of (12) and (14) are obtained by multiplying each set by the conduction angle i.e. D and $1-D$ and adding the result so as to obtain (15) and (16) respectively.

$$\begin{pmatrix} \dot{i}_L \\ \dot{v}_c \end{pmatrix} = \begin{pmatrix} 0 & \frac{d-1}{nL} \\ \frac{1-d}{nC} & -\frac{1}{RC} \end{pmatrix} \begin{pmatrix} i_L \\ v_c \end{pmatrix} + \begin{pmatrix} \frac{d}{L} \\ 0 \end{pmatrix} v_{in} \qquad \ldots(15)$$

$$v_o = \begin{pmatrix} 0 & 1 \end{pmatrix} \begin{pmatrix} i_L \\ v_c \end{pmatrix} \qquad \ldots(16)$$

Linearizing (15) and (16) results in:

$$\begin{pmatrix} \dot{\hat{i}}_L \\ \dot{\hat{v}}_c \end{pmatrix} = \begin{pmatrix} 0 & \frac{D-1}{nL} \\ \frac{1-D}{nC} & -\frac{1}{RC} \end{pmatrix} \begin{pmatrix} \hat{i}_L \\ \hat{v}_c \end{pmatrix} + \begin{pmatrix} \frac{v_c + nv_{in}}{nL} & \frac{D}{L} \\ -\frac{i_L}{nC} & 0 \end{pmatrix} \begin{pmatrix} \hat{d} \\ \hat{v}_{in} \end{pmatrix} \qquad \ldots(17)$$

$$v_o = \begin{pmatrix} 0 & 1 \end{pmatrix} \begin{pmatrix} i_L \\ v_c \end{pmatrix} \qquad \ldots(18)$$

The transfer function of (17) and (18) is obtained by using the state space to transfer function relationship

$$T_S = C(SI - A)^{-1} B$$

Hence the transfer function of the converter was obtained as:

$$\frac{\hat{v}_o(s)}{\hat{d}(s)} = \frac{i_L}{nC}\left[\frac{\frac{(v_c + nv_{in})(1-D)}{i_L nL} - s}{s^2 + \frac{s}{RC} + \frac{(D-1)^2}{n^2 CL}}\right] \quad \ldots(19)$$

Referring the schematic of Fig.4 the transfer function of the Optocoupler is obtained as;

$$\frac{\hat{v}_f}{\hat{v}_o} = \frac{CTR\beta R_E}{R_f} \quad \ldots(20)$$

Where CTR is the optocoupler current transfer ratio.

The PWM is an open loop high gain error amplifier which compares a reference high frequency ramp voltage with the error signal obtained from the error amplifier to generate high frequency pulses of required duty cycle to drive the power switch of the converter. When the error signal $e(t)$ is below the level of the ramp voltage $r(t)$ a low is generated by the amplifier and a high is generated if the error signal $e(t)$ is above the ramp $r(t)$ as shown in Fig.6.

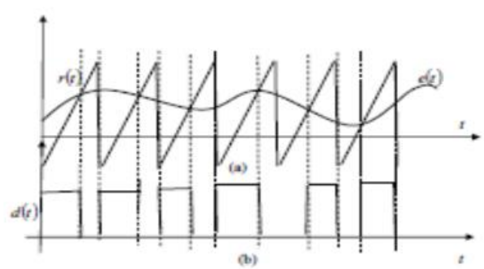

Fig 6: The Pulse Width Modulator Waveform

(a) Ramp and error voltage (b) PWM output

The transfer function of the PWM is obtained using the principle of similar triangle as;

$$\frac{\hat{d}}{\hat{v}_c} = \frac{1}{v_m} \quad \ldots(21)$$

The PI controller is designed by tuning the gains in MATLAB SISOTOOL as shown in Fig.7 to improve the system dynamics performance through pole placement at the origin and zero located at $\omega_z = 500$ rad/s.

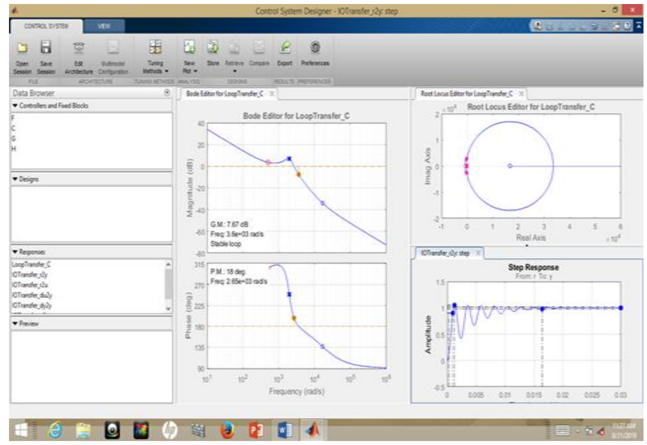

Fig 7: PI Controller Tuning in MATLAB

The transfer function of the PI controller is obtained as;

$$G_C = \frac{0.0018(s + 500)}{s} \quad \ldots(22)$$

Hence the proportional and the integral gain constants are: $k_p = 0.0018$ and $k_i = 0.9$

The DC motor dynamics used for simulation are given as:

$$v_a = L_a \frac{di_a}{dt} + i_a R_a + E_b \quad \ldots(23)$$

$$T_a = T_e - T_L = j\frac{d\omega}{dt} + B\omega \quad \ldots(24)$$

$$v_f = L_f \frac{di_f}{dt} + i_f R_f \quad \ldots(25)$$

D. Complete Flyback Converter Circuit Implementation

The flyback converter circuit implementation in LTspice is shown in Fig.8

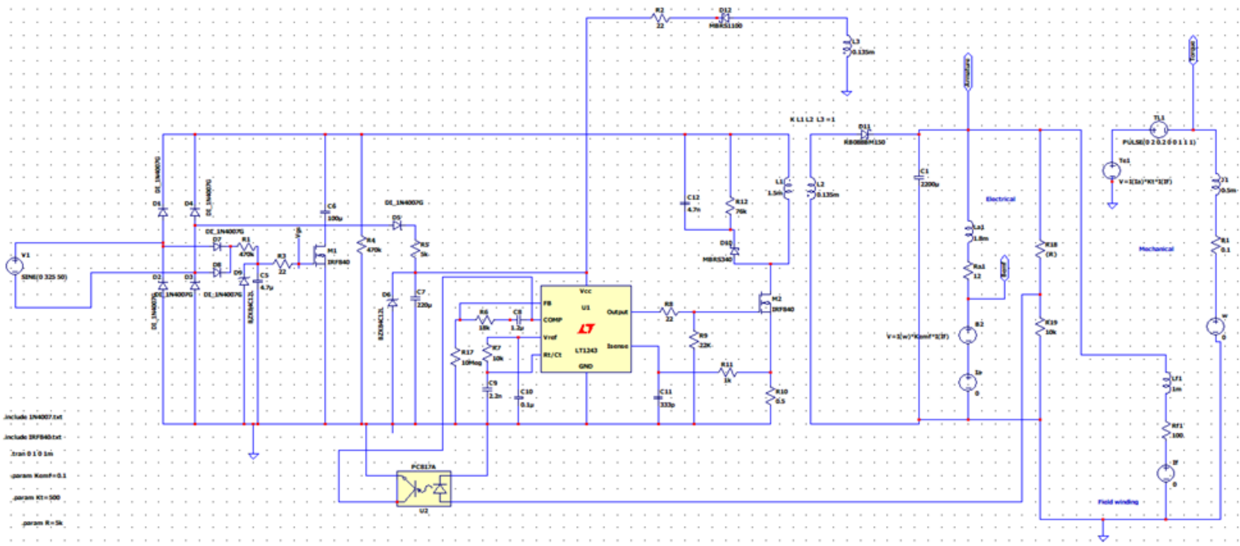

Fig 8: The Complete Flyback Circuit Implementation

III. RESULTS AND DISCUSSIONS

The results presented in this section are simulated in MATLAB and LTspice

Fig.9 shows input mains, AC-DC and converter output. When the input mains are at its peak, the output voltage of the AC-DC converter was at 0V until after a 4V MOSFET gate threshold is reached as shown by the dotted line which correspond to a delay of 35ms at which time, the capacitor start building charge since the MOSFET is ON and provides a small resistance to prevent inrush current through the circuit. When there is a sudden power interruption, the MOSFET quickly switches off and provide a very large resistance to protect the circuit.

Table 4 shows the output of the AC-DC converter when the input voltage is varying from 120V-400V. it is seen that the output of the flyback converter is maintained at 12V, this is so because any variation in the armature voltage will be compared with a reference set by the PI controller so as to give a control signal to vary the duty cycle of the switch thereby keeping the voltage constant. This result was validated by experimentally testing the constructed flyback converter using a Variac to provide a variable input supply for the converter and the output voltage was observed to be constant even when the input was changing.

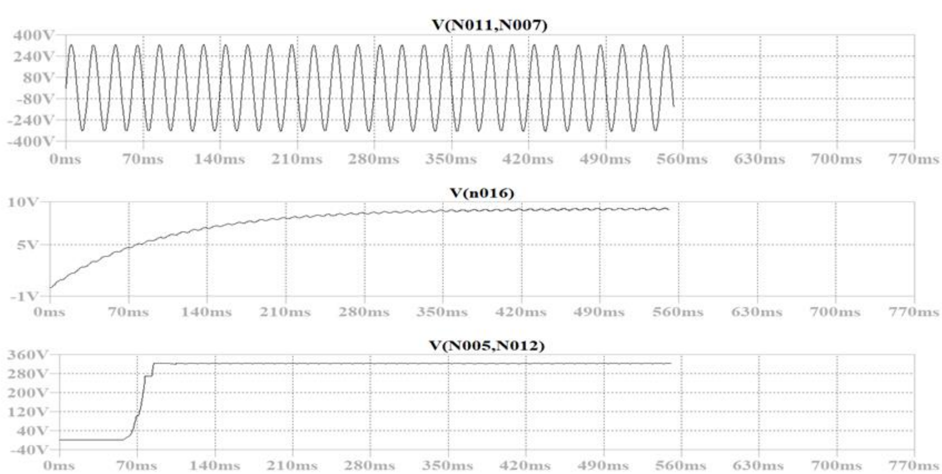

Fig 9: Results for AC-DC Converter with Over Current and Inrush Protection

Table 4: Result of the Flyback Converter

Peak input mains (V)	AC-DC converter (V)	Flyback converter (simulation) (V)	Flyback converter (Experimental) (V)
180	118	11.9	11.8
200	198	12.0	11.9
280	277	12.1	12.2
350	348	12.1	12.2
400	397	12.1	12.4

A. Effect of Variable Armature Voltage on Torque and Speed

The effect of not regulating the output voltage of the flyback converter on the speed and the mechanical torque developed by the DC motor is shown on Fig.10. It is seen that when the armature voltage is allowed to vary by not deploying the controller into action, the mechanical torque developed by the motor changed in response to the varying armature voltage which changes the speed of the motor.

B. Effect of Constant Armature Voltage on Torque and Speed

When the PI controller is deployed to fix the armature voltage at 12V, the mechanical torque developed by the DC motor is maintained constant to ensures that the motor runs at a constant value which is shown in Fig 11.

C. PI Controller Response

The performance index of the PI controller as seen in Fig.12 in time domain analysis (Root locus diagram) shows that a rise time of 0.7ms and a peak overshoot of 5.11% were achieved which corresponds in the frequency domain to a phase margin of 18° and a gain margin of $7.67dB$. This shows a tremendous improvement in desirable performance of the system.

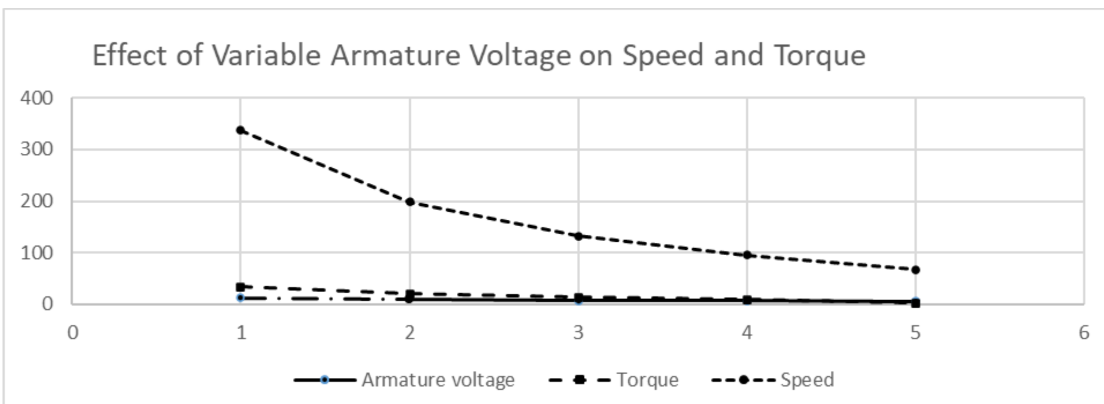

Fig 10: Effect of Variable Armature Voltage on Motor Speed and Torque

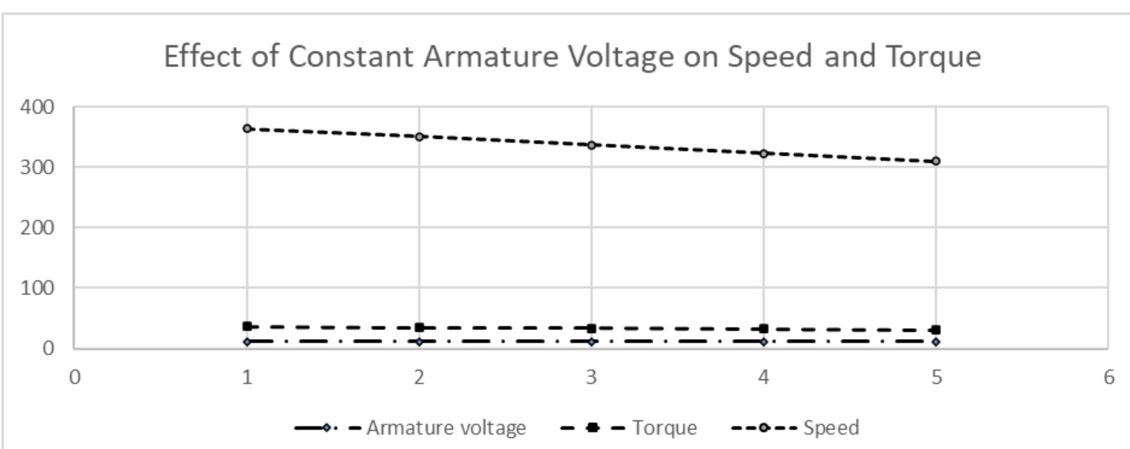

Fig 11: Effect of Fixed Armature Voltage on Motor Speed and Torque

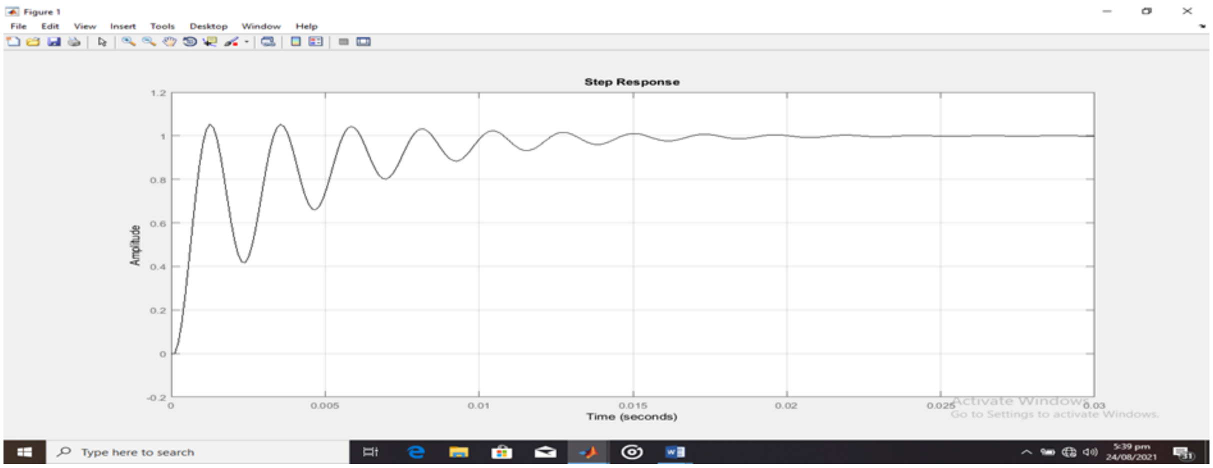

Fig 12: The PI Controller Unit Step Response

SUMMARY AND CONCLUSION

A flyback converter is a non-minimum phase system and needs to be control. In this work, a PI controller was deployed to control a flyback converter for armature DC motor regulation, the effect of deploying the controller to maintained a constant armature voltage was investigated and the effect of not deploying the controller to fixed the armature voltage was also studied. The PI controller was able to give a faster and stable control loop of 0.7ms rise time and 5.11% peak overshoot to ensure that a good control is achieved.

REFERENCES

[1] A. Howard, How to Design DC-DC Converters, Fourth edi. london: McGraw- Hill, 2015.

[2] Rourkela, "Speed Control of DC Motor using Chopper," Int. Conf. Adv. Electr. Eng., 2013.

[3] M. Subramanyam and K. Eswaramma, "Speed Control of Separately Excited Dc Motor Using A High Efficiency Flyback Converter With New Active Clamp Technique," Int. J. Eng. Res. Appl., vol. 4, no. 10, pp. 90–95, 2014, [Online]. Available: www.ijera.com RESEARCH.

[4] T. Jaykumar, "Closed loop Modelling of Flyback Converter for Speed Control of Separately Excited DC Motor," Int. J. Adv. Eng. Res. Dev., vol. 1, no. 3, 2014.

[5] E. E. El-Kholy, "AC / DC Flyback Converter with a Single Switch Controlled DC Motor Drives," IEEE PEDS, pp. 395–400, 2005.

[6] Umanand, Power Electronics Essential and Applications, First edi. John willey, 2009.

[7] M. Ferdowsi et al., "Pulse Regulation Control Technique for Flyback Converter," EEE Trans. POWER Electron., vol. 3, pp. 1745–1750, 2004.

[8] K. Venkateswarlu and C. Chengaiah, "Comparative Study on DC Motor Speed Control using Various Controllers," Glob. J. Res. Eng. Electr. Electron. Eng. Vol., vol. 13, no. 17, pp. 6–11, 2013.

[9] N. Kumar and A. Kasundra, "Design and Simulation of Flyback Converter in MATLAB using PID Controller," Int. J. Latest Res. Sci. Technol., pp. 960–965, 2016, doi: 10.15662/IJAREEIE.2016.0502057.

[10] Manjunatha and Manjesh, "Design and Development of Fly-Back Converter with Buck-Boost Regulator for DC Motor used in Electric Vehicle for the Application of Renewable Energy," Int. Conf. circuits Power Comput. Technol. [ICCPCT] Des., pp. 1–4, 2017.

[11] D. W. Hart, commonly used Power and Converter Equations, Third edi. McGraw-Hill, 2010.